ELSEVIER

Surface Science 366 (1996) 19–28

surface science

Coverage dependence of the kinetics for H_2 desorption from Rh(111)

J.I. Colonell, T.J. Curtiss[1], S.J. Sibener *

The James Franck Institute and Department of Chemistry, The University of Chicago, 5640 S. Ellis Avenue, Chicago IL60615, USA

Received 16 January 1996; accepted for publication 29 April 1996

Abstract

Coverage-dependent sticking probabilities and second-order rate constants for recombinative desorption of hydrogen from Rh(111) have been measured using molecular beam relaxation spectroscopy (MBRS) and time-resolved specular helium scattering. The sticking probability follows second-order Langmuir coverage dependence, with s_0 equal to 0.01 ± 0.005. Under isothermal and nearly isosteric conditions over the coverage range 0.2–0.7 ML, the second-order rate constant for desorption is essentially independent of hydrogen coverage, in contrast to kinetic parameters determined from thermal desorption spectra.

Keywords: Adsorption isotherms; Adsorption kinetics; Hydrogen; Low index single crystal surfaces; Molecule–solid reactions; Rhodium; Sticking; Thermal desorption

1. Introduction

Hydrogen recombination is probably the most widely studied surface reaction, of interest both because of the relative simplicity of modeling it, and for its importance in a number of industrial processes. The kinetics and dynamics of this reaction have been studied on a wide variety of surfaces using many different techniques [1–4]. One of the relatively unexplored corners of this well-studied topic is the effect of hydrogen coverage on the reaction. Interadsorbate interactions are known to have an important effect on the kinetics of many reactions: CO desorption and CO oxidation are two prominent examples [3,5,6]. Modulated molecular beam relaxation spectroscopy (MBRS) studies, which allow measurement of the kinetics at constant temperature and nearly constant coverage, have largely been conducted at very low coverages [7,8]. Temperature-programmed desorption (TPD) studies can access the high coverage regime, but only under conditions of rapidly changing temperature and coverage, which can make the results difficult to interpret.

TPD techniques have been used to study the coverage dependence of H_2 desorption kinetics from a variety of surfaces [1,2]. The only such study of the current system was reported by Yates, Thiel and Weinberg [9] (hereafter YTW). They measured TPD spectra for H_2, D_2 and HD desorbing from Rh(111). Their spectra show two broad, overlapping peaks. Using the method of Chan et al. [10] they find that the effective activation energy

* Corresponding author. Fax: +1 312 7025863; e-mail: sibener@silly.uchicago.edu

[1] Current address: Department of Chemistry, Henry Eyring Building, University of Utah, Salt Lake City, UT 84112.

PII S0039-6028(96)00807-2

for desorption decreases from 18.6 kcal mol^{-1} near zero coverage to just 4 kcal mol^{-1} at 1 ML. Although, as they point out, only effective Arrhenius parameters may be extracted from their data, such a large decrease is still suggestive of strong coverage dependence of the kinetics.

TPD spectra of hydrogen desorbing from Ni(111) [11,12], Pt(111) [13,14], Ir(111) [15] and Ru(001) [16] also show either two peaks or (in the case of Ir(111)) an extremely broad single peak which is suggestive of two peaks. The coverage dependence of the TPD spectra varies. TPD spectra of H_2 desorbing from Ni(111) show two well-resolved peaks which have coverage-independent activation energies of 19 kcal mol^{-1} and 22 kcal mol^{-1} [12]. Christmann et al. analyze their TPD spectra of the H/Pt(111) system as two peaks, and find activation energies of 9.1 and 4.9 kcal mol^{-1} corresponding to the high and low temperature peaks, respectively. Only the activation energy for the high-energy peak is coverage-dependent: it decreases to 6.6 kcal mol^{-1} at a hydrogen coverage of 0.95 ML. However, Poelsema et al. measured adsorption and desorption isotherms on H/Pt(977) and found coverage-independent desorption activation energies of $\sim$20 kcal mol^{-1} on the terraces over their coverage range of zero to 0.5 ML [17]. Engstrom et al. analyze their TPD spectra of H_2 desorbing from Ir(111) by varying the temperature ramp rate and constructing isosteric Arrhenius plots: they find that the activation energy decreases from 18 kcal mol^{-1} at very low coverages to $\sim$10 kcal mol^{-1} at $\theta_H \approx 0.4$ ML [15]. High-resolution TPD spectra of the H/Ru(001) system show that the activation energy for hydrogen desorption decreases from 24 to 12 kcal mol^{-1} as the coverage increases from zero to 1 ML [16].

The general picture which emerges from these studies is that the TPD spectra of hydrogen desorbing from the hexagonal surface of transition metals are generally bimodal and strongly coverage-dependent. The details are less clear. Is the coverage dependence of the kinetics due to changing occupation of two sites which have different desorption kinetics, or is it due to strong repulsive interadsorbate interactions? Of course, both of these factors, and others, may be important, and the answer may be different for each system.

The motivation for the current work was to study the kinetics of hydrogen desorption under nearly steady-state conditions and explore the coverage dependence of desorption in more detail. We measure the kinetics using MBRS combined with time-resolved specular helium scattering to measure the hydrogen coverage on the surface. Using MBRS we can measure the kinetics under isothermal and nearly isosteric conditions. Most MBRS studies detect products desorbing from the surface [7,8]. Measuring coverage waveforms, i.e. the buildup and decay of the hydrogen coverage as the beam is modulated, with He scattering has two advantages over measurement of product waveforms for this system. The first is that it allows us to obtain absolute values of the second-order rate constant (which requires knowledge of the hydrogen coverage). The second is that it alleviates the experimental difficulties of separating desorbed from scattered H_2, and gives a better signal-to-noise ratio than measuring the weak desorbed H_2 signal over the large H_2 background in the detector.

2. Experimental

These experiments were performed in a molecular beam scattering machine which has been described previously [7,18,19]. Only the features essential to these experiments will be described in detail here. The UHV scattering chamber is pumped by a 400 $\ell\ s^{-1}$ ion pump and a titanium sublimation pump. It contains a three-axis crystal manipulator, and an independently rotatable differentially pumped quadrupole mass spectrometer detector. Three continuous molecular beams are formed by supersonic expansion in the source chamber. The three beams are in a plane perpendicular to the scattering plane. The center beam is in the scattering plane defined by the plane of rotation of the detector, and may be modulated upstream from the crystal with a motor-driven chopper. The two side beams are inclined by 15° on either side of the center beam, and all three beams can be modulated at low frequencies (< 1 Hz) by solenoid-

driven beam flags. The beam spots of the side beams at the crystal are ellipses about 5 mm × 7 mm. The center beam spot is ~1.5 mm in diameter. The angular acceptance of the detector is about 1°, slightly larger than the angular spread of the center beam. The intensities of the side beams are measured with ion gauge fluxmeters.

In the waveform measurements, the center beam is always a room-temperature (~63 meV) He beam used to monitor the hydrogen coverage on the surface, and is modulated at 100 Hz to allow background subtraction. A continuous, intense (~1–5 ML s^{-1}) beam of hydrogen in one side beam is used to establish a steady-state coverage. A weaker hydrogen beam (about one-half to one-third the intensity of the continuous beam) in the second side beam modulates the hydrogen coverage on the surface by about 5–10%.

The Rh(111) sample (Cornell Materials Preparation Laboratory) was cut and polished to within 1° of the (111) face and checked by X-ray Laue back-reflection. The primary contaminants were S, B, and C. S and B were removed by cycles of Ar^+ sputtering (10 μA, 900 K) followed by annealing at 1300 K. C was removed daily by exposing the crystal to oxygen at 900 K and annealing at 1300 K. Cleanliness was checked by Auger spectroscopy, and surface flatness by He reflectivity.

3. Results and discussion

3.1. Calibration of the He reflectivity versus hydrogen coverage

Specular He scattering has long been known to be very sensitive to the presence and concentration of adsorbates on metal surfaces [20]. Poelsema and Comsa have exploited this property of the He reflectivity to study a variety of surface phenomena [21]. It has also been used in our group with MBRS to measure the coverage-dependent kinetics of CO desorption [6].

To determine the dependence of the specular He reflectivity on hydrogen coverage on Rh(111), we first measured an adsorption isotherm, i.e. the dependence of the coverage on hydrogen exposure. We then correlated this data with the dependence of the He reflectivity on hydrogen exposure.

We measured the adsorption isotherm by measuring the integrated HD thermal desorption signal as a function of exposure to a mixed H_2/D_2 beam. We used mixed overlayers of hydrogen and deuterium in these experiments simply to take advantage of the low mass three background in our detector: YTW [9] found that TPD spectra were identical for hydrogen, deuterium, and mixed overlayers. The measured isotherm was converted to a coverage versus exposure curve by dividing by the integrated HD desorption signal from a saturated overlayer, formed by dosing at 160 K, which showed a (1 × 1) He diffraction pattern. The result is shown in Fig. 1a. A saturated overlayer on Rh(111) is known from LEED and helium scattering studies to have a (1 × 1) structure with one atom per Rh unit cell, and hence is a full monolayer [9,22,23]. It is straightforward to distinguish the ordered (1 × 1) hydrogen overlayer from diffraction from the Rh surface using He scattering: the much higher corrugation of the hydrogen overlayer results in first-order diffraction peaks which are a factor of 10–20 larger than those from the Rh surface [23]. The different symbols in Fig. 1a correspond to different temperatures and beam fluxes, indicating that the adsorption isotherm, within our experimental error, does not depend on these variables. These adsorption curves do not extend to saturation because, at very high coverages, hydrogen desorbs at surface temperatures above 160 K. Fig. 1b shows $(-\ln(\theta))$ plotted as a function of the hydrogen exposure, while Fig. 1c shows $\theta/(1-\theta)$. In agreement with YTW, [9], the latter is linear, showing that adsorption follows second-order Langmuir kinetics, i.e. the sticking probability is given by

$$s(\theta) = s_0(1-\theta)^2, \quad (1)$$

where s_0 is the zero-coverage sticking coefficient. The sticking coefficient is determined from the linear fit in Fig. 1c to be 0.01 ± 0.005. YTW measured a sticking coefficient of 0.65 from their Langmuir isotherm. The disagreement could be due to differences between dosing from a supersonic beam and from the thermal background, or differences in the surface: H_2 sticking coefficients

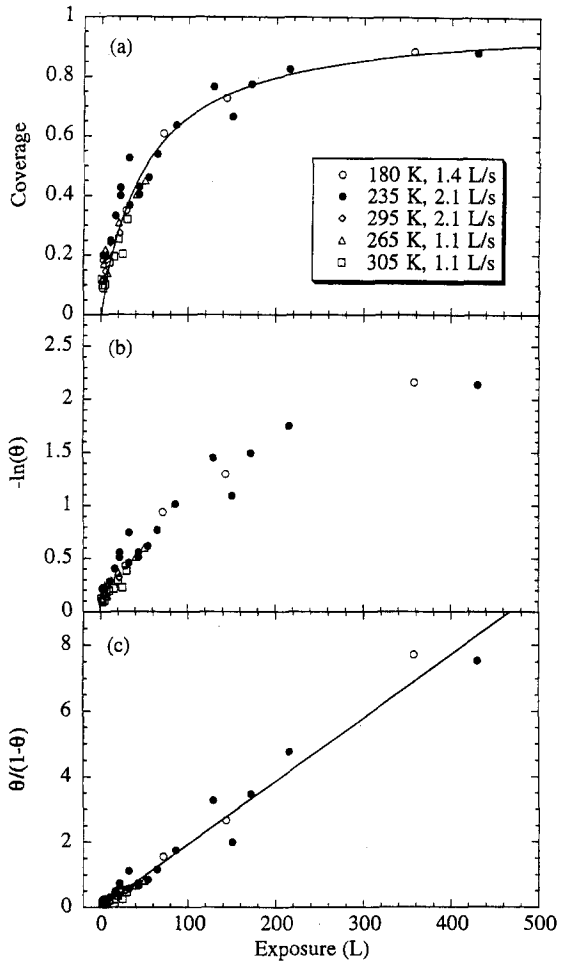

Fig. 1. (a) Adsorption isotherm at various temperatures and fluxes as labeled. (b) $-\ln(\theta)$, which should be linear for first order adsorption. (c) $\theta/(1-\theta)$, which is linear for second-order adsorption.

are often sensitive to surface quality [21,24]. Other transition-metal surfaces show zero-coverage H_2 sticking coefficients of ~ 0.01 or lower, including Ni(111) [24], Pt(111) [21,25] and Ir(111) [15].

The dependence of the specular helium reflectivity on hydrogen exposure was measured simply by monitoring the He signal while dosing with a hydrogen beam. We found that the dependence of the He reflectivity on exposure to H_2, D_2, and mixed H_2/D_2 beams of the same intensity are essentially identical. The coverage as a function of exposure was then calculated from the isotherm in Fig. 1, yielding the He reflectivity versus coverage curves shown in Fig. 2. The incident and final angles in this measurement, and in the later waveform measurements, were 45°. The dependence of the reflectivity on coverage is qualitatively similar to that determined for the much studied H/Pt(111) system [21,26]: the He reflectivity decreases rapidly at low coverages and recovers at higher coverages. We found that for the H/Rh(111) system, as for H/Pt(111), the depth of the minimum is dependent on the incident angle. Poelsema and Comsa [21] have developed a detailed model for the H/Pt(111) system, which explains the U-shaped curve in terms of diffuse elastic scattering of He by isolated hydrogen adatoms and vacancies in the H overlayer, and interference between He specularly scattered from the clean surface and the overlayer. According to this model, the depth of the minimum changes as the interference between He scattered from the metal surface and the overlayer changes from constructive to destructive. The general explanation of the H/Rh(111) system may be similar, but the position of the minimum (at a hydrogen coverage of about 0.05 ML instead of the 0.5 ML found for H/Pt(111)) and the curvature of the reflectivity versus hydrogen coverage at high coverages are substantially different. The discrepancy could be due to differences in the phase diagram for H/Rh(111), or perhaps adsorption at surface defects. The reflectivity of the clean Rh(111) surface at 500 K is $\sim 20\%$, indicating that the surface is well ordered and smooth, but the defect density

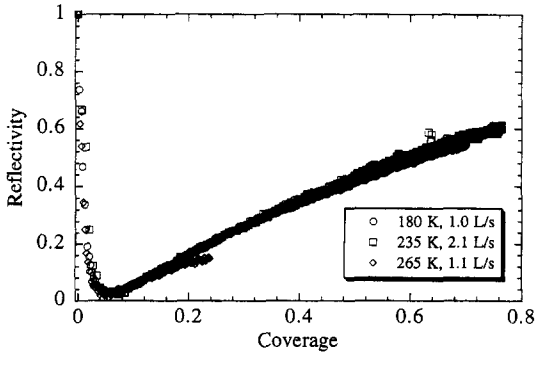

Fig. 2. He reflectivity plotted as a function of hydrogen coverage at various temperatures and fluxes as labeled. The reflectivity of the clean surface at the experimental temperature is set equal to one for each.

is certainly larger 0.001, the measured defect density of the platinum crystal used in the experiments of Poelsema and Comsa [21]. Since we were unable to fit our data with the Poelsema–Comsa model, we fit the data in Fig. 2 to an arbitrary form, and calculated the coverage from that. We corrected for the temperature dependence of the reflectivity by setting the reflectivity of the clean surface at the measurement temperature equal to one. This is equivalent to scaling the whole curve with the Debye–Waller factor for the clean surface. That is, the reflectivities in Fig. 2 are given by

$$\text{Reflectivity}(\theta_H, T_s) = \frac{I(\theta_H, T_s)}{I(0, T_s)} = \frac{I(\theta_H, T_s)}{I(0,0)\exp(-DT_s)}, \tag{2}$$

where D is determined from the measured temperature dependence of the He reflectivity of our Rh(111) surface. This also happens to correct for the temperature dependence of the He reflectivity of the hydrogen overlayer, because the Debye–Waller factors for the clean Rh surface and the overlayer are very similar: for both, D is $\sim 0.0027\ \mathrm{K}^{-1}$. As can be seen from Fig. 2, the He reflectivity of partial overlayers is independent of temperature apart from this Debye–Waller correction, indicating that the coverage calibration is not complicated by phase transistions or islanding effects in the overlayer in the temperature range of our kinetic measurements. In practice, we measured the clean surface reflectivity at 600 K to avoid contamination of the surface by carbon monoxide and hydrogen from the chamber, and extrapolated that value to the working temperature using the Debye–Waller factor.

3.2. Hydrogen desorption kinetics

To measure the desorption kinetics using MBRS, we created a steady-state coverage with an intense H_2 beam, and perturbed that coverage with a weaker H_2 beam modulated by a beam flag. The coverage was monitored continuously by measuring the He reflectivity. Assuming that H_2 desorption is second order, the equation for the hydrogen coverage as a function of time is

$$\frac{d\theta_H}{dt} = 2s_0(1-\theta_H)^2 F(t) - 2k_2(\theta_H, T_s)\theta_H^2, \tag{3}$$

where k_2 is the second-order rate constant. $F(t)$, the hydrogen flux as a function of time, is the flux of the intense beam plus a square wave created by the modulation of the weak beam. If the modulation is weak enough, then the differential equation (Eq. (3)) can be linearized, and the methods of Fourier analysis may be used to extract rate constants from the coverage waveforms [7,8,27–29]. However, this linear limit is extremely difficult to achieve for a second order reaction, where the nonlinearity is more than simply a coverage-dependent rate constant, or even the coverage change of a second reactant; here there are two squared terms in the differential equation. Simulations of waveforms show that coverage modulations of about 1% are needed to fully linearize the response to the perturbation.

Such small coverage modulations are beyond our ability to measure reliably. We found for this system that coverage modulations of 5–10% were necessary to obtain adequate signal-to-noise ratios in a reasonable time. The waveform measurements still have the advantage of being isothermal and of creating only small coverage changes during the measurement, so that the second-order rate constant may be assumed to be nearly constant, but the rate constants can not be determined using Fourier analysis. We chose to fit the waveforms to an analytic solution of the second-order kinetics.

If the flux is constant, the nonlinear differential equation for the coverage given in Eq. (3) is an inhomogeneous Ricatti equation, the solution of which may be found in textbooks on differential equations. Briefly, we make the substitution

$$z(t) = \theta_H(t) + p(t), \tag{4}$$

where $p(t)$ is a particular solution to the differential equation. If we choose the solution to the steady-state equation, where $\frac{d\theta_H}{dt}$ is zero and $p(t)$ is a constant defined by the equation

$$Fs_0(1-p)^2 = k_2 p^2, \tag{5}$$

substituting z into Eq. (3) yields, after some simplification

$$\frac{dz}{dt} = 2k_2\left(\frac{Fs_0}{k_2} - 1\right)z^2 + 2k_2 \times\left[\left(\frac{Fs_0}{k_2} - 1\right)p - \frac{Fs_0}{k_2}\right]z. \quad (6)$$

The differential equation is now in the form of the Bernoulli equation, which may be transformed into a linear ordinary differential equation with the substitution $z = 1/w$. Since the solution only applies where the flux is constant, it is solved separately for the two parts of the square wave, with the weak beam on and off. If the waveform is not overmodulated, so that the coverage reaches its steady-state with the beam on and off in each cycle, then the steady-state solutions (i.e. the steady-state coverages) are known from the coverage waveform, and it is not necessary to measure the beam fluxes or the sticking coefficient (since the product Fs_0 is determined from Eq. (5)). Some experimental coverage waveforms and fits to this solution are shown in Fig. 3, and the second-order rate constants extracted are shown by the open symbols in Fig. 4. One persistent difficulty in these measurements was the coadsorption of CO from the chamber background, which perturbs the He scattering even at very low CO coverages due to its large diffuse elastic cross-section [6,21]. We compensated by frequently flashing the crystal to remove adsorbed CO and subtracting off the sloping baseline of the reflectivity waveforms, but this problem may account for the scatter in the rate constants in Fig. 4.

We checked these rate measurements using our ability to measure the beam fluxes and our measurement of the zero-coverage sticking coefficient. When these quantities are known, the second-order rate constant may be measured under true steady-state conditions, with a single constant beam of H_2 and a He beam to measure the reflectivity and hence the coverage. The second-order rate constant may then be calculated from Eq. (5), where p is the measured coverage: the results are shown by the solid symbols in Fig. 4. These rate constants can only be as accurate as the fluxmeters, so may be off by 20–30%, but are certainly in reasonable agreement with the waveform measurements.

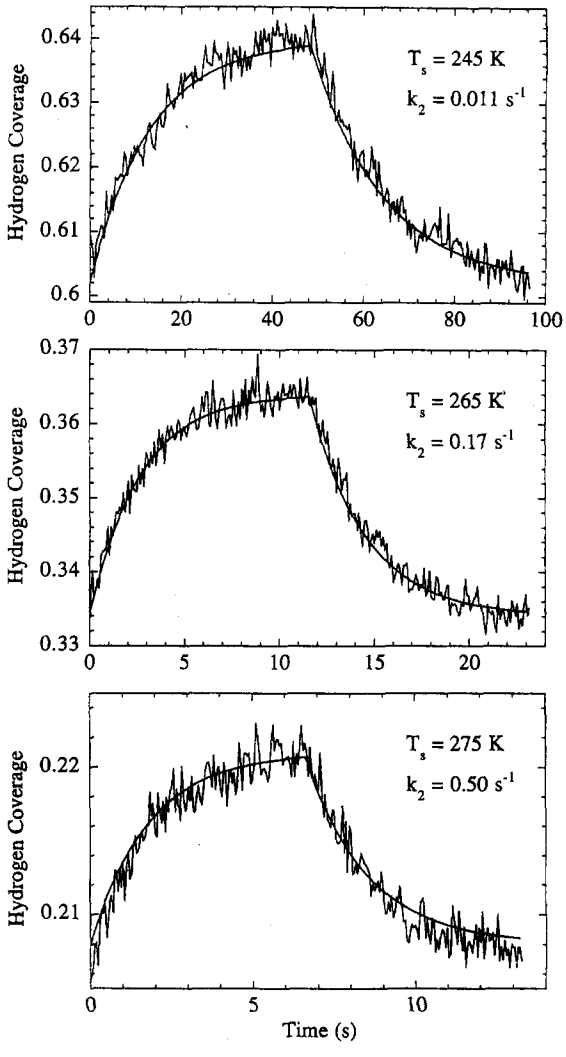

Fig. 3. Hydrogen coverage waveforms at three temperatures. The solid lines are fits are to the solution of Eq. (3).

From Fig. 4, the second-order rate constant appears to be essentially independent of coverage, although the large scatter may conceal a weak coverage dependence. We constructed an Arrhenius plot by simply taking the mean at each temperature, assuming that k_2 is independent of coverage. The result is shown in Fig. 5. The activation energy and pre-exponential factor obtained are 17 ± 2 kcal mol^{-1} and $3 \times 10^{13} \pm 2 \times 10^{13}$ s^{-1} ($2 \times 10^{-2} \pm 1 \times 10^{-2}$ cm^2 s^{-1}). The Arrhenius

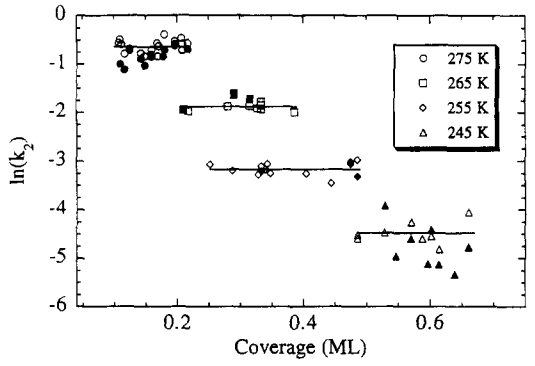

Fig. 4. Second-order rate constants plotted as a function of hydrogen coverage. The open symbols are rate constants obtained from waveforms, and the filled symbols are values obtained from steady-state measurements. The solid lines show the mean rate constant determined at each surface temperature: k_2 (275 K)=0.53 s^{-1}; k_2 (265 K)=0.15 s^{-1}; k_2 (255 K)=0.042 s^{-1}; k_2 (245 K)=0.011 s^{-1}.

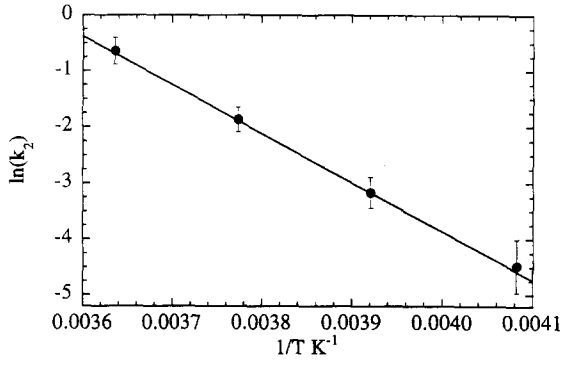

Fig. 5. Arrhenius plot of the average rate constants measured at each temperature.

parameters obtained by YTW from low coverage TPD measurements are $E_a = 18.6$ kcal mol^{-1} and $A = 1.9 \times 10^{12}$ s^{-1} (1.2×10^{-3} $cm^2 s^{-1}$) [9]. From low-coverage HD waveforms Padowitz and Sibener [8] found $E_a = 20$ kcal mol^{-1} and $A = 2 \times 10^{13}$ s^{-1} (10^{-2} cm^2 s^{-1}). The agreement of our parameters with these previous results is reasonable, especially given the limited temperature range of our measurements.

3.3. Comparison with TPD measurements

The majority of data concerning the coverage dependence of desorption rate constants has been obtained from TPD measurements, observing the position and width of the TPD peak as a function of initial coverage. TPD spectra for this system, obtained by dosing with a mixed H_2/D_2 beam at 140 K and monitoring the HD signal as the temperature is ramped at about 7 K s^{-1}, are shown in Fig. 6a. The position and width of the TPD peak are similar to those in the TPD spectra measured by YTW [9], although the spectra in Fig. 6a are more clearly bimodal. Fig. 6b compares the experimental TPD spectra (dashed lines) with calculated spectra which assume that the second-order rate constant is independent of coverage, and that is temperature dependence may be calculated from the Arrhenius parameters determined in Fig. 5. The exact position of the peak is fairly sensitive to the Arrhenius parameters and may not be quite correct: in particular, the fact that the calculated spectra line up with the low-temperature peak may be a coincidence. However, the general conclusion is clear: as noted by YTW in Fig. 7 of

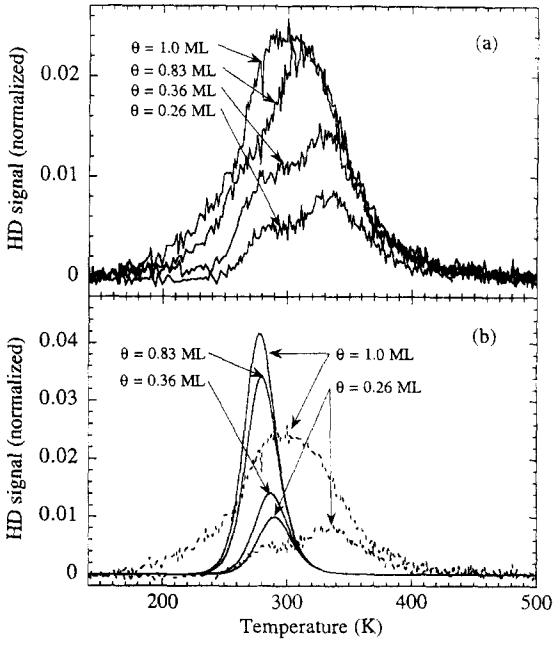

Fig. 6. (a) TPD spectra, showing HD desorption signal as a function of temperature. The surface was dosed at 140 K, and the ramp rate was ~7 K s^{-1}. The initial coverages for each spectrum are labeled. (b) Comparison of the measured TPD spectra (dashed lines) with calculated spectra using the Arrhenius parameters obtained from Fig. 4.

Ref. [9], the measured TPD spectra cannot be reproduced by a coverage-independent, or even weakly coverage-dependent, rate constant. The effective Arrhenius parameters determined by YTW from their TPD spectra yield rate constants that change by two to three orders of magnitude as the coverage changes from 0.1 to 0.7 ML; such a strong coverage dependence would be clearly apparent in our measurements.

The difference between our kinetic measurements and the TPD spectra is somewhat puzzling. The most obvious interpretation of strongly coverage-dependent TPD spectra is a coverage-dependent rate constant, usually due to interadsorbate interactions. Meng and Weinberg [30,31] have shown with Monte Carlo and quasichemical calculations that repulsive interadsorbate interactions may even lead to multiple peaks in TPD spectra. However, most of the available data concerning the H/Rh(111) system do not suggest large interadsorbate interactions. As mentioned earlier, the only ordered structure observed using LEED is the (1×1) at 1 ML coverage [9,22]. We also observed the (1×1) structure using He diffraction, and looked for (2×2) and $(\sqrt{3} \times \sqrt{3})$ structures (which have been observed for hydrogen overlayers on other metal surfaces [1]) without finding them, suggesting that the interadsorbate interactions are relatively small. Experimental measurements have shown that the rate of surface diffusion of hydrogen on Rh(111) is independent of coverage [32,33], also indicating that the interadsorbate interactions are weak. Finally, while Meng and Weinberg's modeling of TPD spectra for adsorbates with large repulsive interadsorbate interactions suggest that the high-coverage spectra are bimodal, they also show that the low-coverage spectra should have only a single peak: the second peak grows in due to high-energy, high-coverage configurations present only at high coverages. The TPD spectra for this system, on the other hand, appear to be bimodal even at low coverages, suggesting that repulsive interadsorbate interactions may not be the correct interpretation. Our data showing that the rate constant for hydrogen desorption is not strongly dependent on the coverage adds to this substantial body of evidence that interadsorbate interactions in this system are weak, and that the strong coverage dependence of the TPD spectra must be due to other factors.

One of those factors could be that the TPD measurements are not conducted under quasi-equilibrium conditions. An important assumption made in the analysis of TPD spectra is that the diffusion of adsorbates is fast enough that an "equilibrium" configuration is formed as quickly as the temperature changes. Hydrogen and deuterium diffusion on Rh(111) is very fast (Mann et al. measured diffusion coefficients of 5×10^{-7} cm^2 s^{-1} at 200 K [32]), so it seems unlikely that the system could be far from equilibrium, even at temperature ramp rates of 7 K s^{-1}. The assumption may be tested experimentally by measuring TPD spectra at a lower ramp rate. TPD spectra at a ramp rate of 2 K s^{-1} are shown Fig. 7. They are somewhat narrower than those at the higher ramp rate, as expected, and the lower coverage spectrum is not as clearly bimodal, but they are qualitatively similar. It seems likely that the system is maintained close to quasi-equilibrium, even at the higher ramp rate.

Another possibility is that there are two distinct adsorption sites on the surface, which give rise to the two peaks in the TPD spectra. Calculations using the embedded cluster method have shown that hydrogen may bind in either the fcc or hcp three-fold sites on the Rh(111) surface, and that the fcc site is more stable by ~2.4 kcal mol^{-1} [34]. Mann et al. have pointed out that if the occupation of these two sites were coverage-dependent, they could account for the coverage depen-

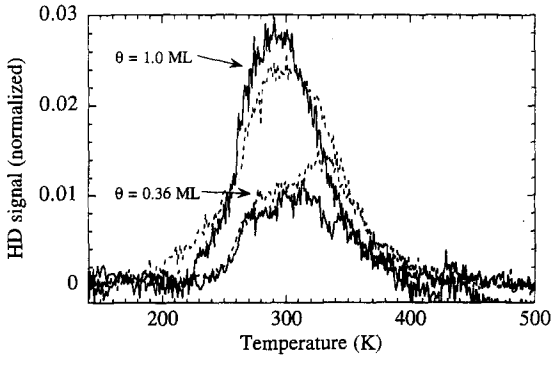

Fig. 7. Comparison of TPD spectra with ramp rates of 2 K s^{-1} (solid lines) and 7 K s^{-1} (dashed lines).

dence of the TPD spectra [32]. None of the coverage waveforms appear to be bimodal, which would be expected if desorption were occurring from two different sites with different binding energies. The rate constants do not show the coverage dependence one might expect, as desorption shifts from mostly one site to the other. It is possible that at low temperatures H_2 desorption is dominated by desorption from a single site – the site corresponding to the low-temperature peak in the TPD spectrum. Another possibility is that the second site is only occupied when the surface is dosed at low temperatures: the surface was dosed at 140 K for the TPD measurements, and at temperatures greater than 245 K for the steady-state measurements. An interesting complement to this work would be a thorough TPD study including different ramp rates to confirm that the quasi-equilibrium condition is being met, and different dosing temperatures to determine if site occupancy is temperature-dependent.

4. Conclusion

We have measured the sticking coefficient for H_2 on Rh(111) and the hydrogen-coverage dependence of the specular helium reflectivity. The zero-coverage sticking coefficient determined is 0.01 ± 0.005. We have used this information to measure the coverage dependence of the second-order rate constant for recombinative desorption of H_2 using time-resolved specular helium scattering and steady-state measurements. Within our error, the rate constant is independent of hydrogen coverage, indicating that interadsorbate interactions are relatively weak for this system. The activation energy and pre-exponential factor obtained are 17 ± 2 kcal mol^{-1} and $3 \times 10^{13} \pm 2 \times 10^{13}$ s^{-1} ($2 \times 10^{-2} \pm 1 \times 10^{-2}$ $cm^2 s^{-1}$). The discrepancy between these measurements and TPD spectra may be due to the presence of two distinct adsorption sites of H on Rh(111), only one of which is probed by our low-temperature, isothermal, nearly isosteric, kinetic measurements.

Acknowledgements

J.I.C. acknowledges financial support from AT and T Bell Laboratories through the Graduate Research Program for Women. Acknowledgement is made to the donors of The Petroleum Research Fund, administered by the ACS, for partial support of this research. Additional support from the NSF Materials Research Science and Engineering Center at The University of Chicago is also gratefully acknowledged.

References

[1] K. Christmann, Surf. Sci. Rep. 9 (1988) 1.
[2] K. Christmann, Mol. Phys. 66 (1989) 1.
[3] T. Engel and G. Ertl, in: The Chemical Physics of Solid Surfaces and Heterogeneous Catalysis, Eds. D.A. King and D.P. Woodruff (Elsevier, New York, 1982).
[4] G. Comsa and R. David, Surf. Sci. Rep. 5 (1985) 145.
[5] T. Engel and G. Ertl, Adv. Catal. 28 (1979) 1.
[6] K.A. Peterlinz, T.J. Curtiss and S.J. Sibener, J. Chem. Phys. 95 (1991) 6972.
[7] D.F. Padowitz and S.J. Sibener, Surf. Sci. 254 (1991) 125.
[8] D.F. Padowitz and S.J. Sibener, J. Vac. Sci. Technol. 9 (1991) 2289.
[9] J.T. Yates, P.A. Thiel and W.H. Weinberg, Surf. Sci. 84 (1979) 427.
[10] C.-M. Chan, R. Aris and W.H. Weinberg, Appl. Surf. Sci. 1 (1978) 360.
[11] K. Christmann, O. Schober, G. Ertl and M. Neumann, J. Chem. Phys. 60 (1974) 4528.
[12] K. Christmann, R.J. Behm, G. Ertl, M.A. Van Hove and W.H. Weinberg, J. Chem. Phys. 70 (1979) 4168.
[13] K. Christmann, G. Ertl and T. Pignet, Surf. Sci. 54 (1975) 365.
[14] D.M. Collins and W.E. Spicer, Surf. Sci. 69 (1977) 85.
[15] J.R. Engstrom, W. Tsai and W.H. Weinberg, J. Chem. Phys. 87 (1987) 3104.
[16] P. Feulner and D. Menzel, Surf. Sci. 154 (1985) 465.
[17] B. Poelsema, G. Mechtersheimer and G. Comsa, Surf. Sci. 111 (1981) 519.
[18] K.D. Gibson and S.J. Sibener, J. Chem. Phys. 88 (1988) 7862.
[19] J.I. Colonell, K.D. Gibson and S.J. Sibener, J. Chem. Phys. 103 (1995) 6677.
[20] D.L. Smith and R.P. Merrill, J. Chem. Phys. 52 (1970) 5861.
[21] B. Poelsema and G. Comsa, Scattering of Thermal Energy Atoms (Springer, Berlin, 1989).
[22] D.G. Castner, B.A. Sexton and G.A. Somorjai, Surf. Sci. 71 (1978) 519.

[23] G. Witte, J.P. Toennies and C. Wöll, Surf. Sci. 323 (1995) 228.
[24] K.D. Rendulic, A. Winkler and H.P. Steinrück, Surf. Sci. 185 (1987) 469.
[25] A.C. Luntz, J.K. Brown and M.D. Williams, J. Chem. Phys. 93 (1990) 5240.
[26] J. Lee, J.P. Cowin and L. Wharton, Surf. Sci. 130 (1983) 1.
[27] H.H. Sawin and R.P. Merrill, J. Vac. Sci. Technol. 19 (1981) 40.
[28] C.T. Foxon, M.R. Boudry and B.A. Joyce, Surf. Sci. 44 (1974) 69.
[29] J.A. Schwartz and R.J. Madix, Surf. Sci. 46 (1974) 317.
[30] B. Meng and W.H. Weinberg, J. Chem. Phys. 102 (1995) 1003.
[31] B. Meng and W.H. Weinberg, J. Chem. Phys. 100 (1993) 5280.
[32] S.S. Mann, T. Seto, C.J. Barnes and D.A. King, Surf. Sci. 261 (1992) 155.
[33] E.G. Seegbauer, A.C.F. Kong and L.D. Schmidt, J. Chem. Phys. 88 (1988) 6597.
[34] J. Muscat, Phys. Rev. B 33 (1986) 8136.